

## SIMULATION OF OFFSHORE WIND TURBINE RESPONSE FOR EXTREME LIMIT STATES

**P. Agarwal**

Dept. of Civil, Arch., and Env. Engineering  
University of Texas  
Austin, TX 78712, USA  
Email: pargarwal@mail.utexas.edu

**L. Manuel**

Dept. of Civil, Arch., and Env. Engineering  
University of Texas  
Austin, TX 78712, USA  
Email: lmanuel@mail.utexas.edu

### ABSTRACT

When interest is in estimating long-term design loads for an offshore wind turbine using simulation, statistical extrapolation is the method of choice. While the method itself is rather well-established, simulation effort can be intractable if uncertainty in predicted extreme loads and efficiency in the selected extrapolation procedure are not specifically addressed. Our aim in this study is to address these questions in predicting blade and tower extreme loads based on stochastic response simulations of a 5 MW offshore turbine. We illustrate the use of the peak-over-threshold method to predict long-term extreme loads. To derive these long-term loads, we employ an efficient inverse reliability approach which is shown to predict reasonably accurate long-term loads when compared to the more expensive direct integration of conditional load distributions for different environmental (wind and wave) conditions. Fundamental to the inverse reliability approach is the issue of whether turbine response variability conditional on environmental conditions is modeled in detail or whether only gross conditional statistics of this conditional response are included. We derive design loads for both these cases, and demonstrate that careful inclusion of response variability not only greatly influences long-term design load predictions but it also identifies different design environmental conditions that bring about these long-term loads compared to when response variability is only approximately modeled. As we shall see, for this turbine, a major source of response variability for both the blade and tower arises from blade pitch control actions due to which a large number of simulations is required to obtain stable distribution tails for the turbine loads studied.

### INTRODUCTION

Statistical extrapolation of extreme loads is being increasingly used in the design of offshore wind turbines

against ultimate limit states, and a recent draft [1] of design guidelines from the International Electrotechnical Commission (IEC) also recommends its use. Statistical extrapolation involves integration of the distribution of turbine loads given specified environmental states with the likelihood of occurrence of the different environmental states; the (conditional) load distributions are obtained by means of turbine response simulations.

While extrapolation methods are relatively better understood for onshore wind turbines [e.g., 2-4], they present several challenges for offshore turbines. For one, the offshore environment involves, as a minimum, the consideration of waves in addition to wind; hence, the number of random variables describing the environment increases. As a result, the domain of integration increases and it can often become impractical to perform computationally expensive simulations over the entire domain if one uses the basic extrapolation approach that involves direct integration. It is thus of interest to explore efficient alternative extrapolation techniques for offshore wind turbine design. A second challenge is that extrapolation of turbine loads needs to recognize the dependence on two (or more) random processes representing the environment—wind and waves, say—each of which influence turbine loads in distinct ways. Several studies in recent years have focused on the complexity of these issues in the offshore environment and have addressed comparisons of alternative methods to extract turbine load extremes [5], possible reduction in simulation effort by careful selection of critical environmental states [6], use of the environmental contour method [7], and use of a suitable percentile of the wave-related random variable (conditional on wind speed) in lieu of the full joint wind-wave distribution [8].

On related matters to those highlighted in these previous efforts, we attempt here to answer several open questions regarding how the peak-over-threshold method should be used

with environmental contour method; whether or not the environmental contour method, which requires considerably less simulation effort is as accurate as direct integration in statistical load extrapolation; and whether or not variability in turbine loads must be carefully accounted for in order to yield accurate long-term design loads. To address these issues, we derive design loads using a model of a utility-scale 5MW offshore wind turbine that was developed at the National Renewable Energy Laboratory (NREL), and assumed to be sited in 20 meters of water. Stochastic time-domain simulations of turbine response form the basis for this study. While the inflow turbulence describing the wind field is simulated using similar procedures to those for onshore turbines, excitation from waves is simulated assuming simplified linear irregular wave kinematics that may not be suitable for this shallow-water site.

The outline of this work is as follows: after describing the extrapolation methods and the simulation model, we examine turbine response statistics for several representative environmental conditions. We then discuss application of the peak-over-threshold (POT) method to derive probability distributions of turbine loads. We illustrate how long-term loads can be derived using the environmental contour (EC) method, first by omitting and then by accounting for turbine load variability (given environmental state). Comparison of these EC-based design load predictions with those obtained by direct integration is discussed. We also discuss how turbine control actions influence variability in long-term loads. Finally, we compare predictions of rare (long-term) load fractiles based on the POT and global maxima methods.

## LOAD EXTRAPOLATION METHODS

Design Load Case 1.1b of the IEC 61400-3 draft design guidelines recommends the use of statistical extrapolation methods to predict extreme turbine loads [1]. Direct integration and the EC method are two common extrapolation methods. These are discussed briefly next.

In direct integration which is most often employed in statistical extrapolation for wind turbine extreme loads, one seeks to estimate the turbine design load,  $l_T$ , associated with an acceptable failure probability,  $P_T$ , or equivalently with a target service life of  $T$  years, using the following equation:

$$P_T = P[L > l_T] = \int_{\mathbf{X}} P[L > l_T | \mathbf{X} = \mathbf{x}] f_{\mathbf{X}}(\mathbf{x}) d\mathbf{x} \quad (1)$$

where  $f_{\mathbf{X}}(\mathbf{x})$  is the joint probability density function of the environmental random variables,  $\mathbf{X}$ . For different trial values of load,  $l_T$ , Eq. (1) enables one to compute the long-term probability of exceeding that load by integrating the short-term load exceedance probability conditional on  $\mathbf{X}$ ,  $P[L > l_T | \mathbf{X} = \mathbf{x}]$ , with the relative likelihood of different environmental conditions,  $\mathbf{X}$ . This method, while exact, is generally expensive as one is required to integrate over the entire domain of all random variables; moreover, the load level,  $l_T$ , is adjusted until the target probability,  $P_T$ , results

from the integration. In this study, two environmental random variables comprise  $\mathbf{X}$  and are taken to be the ten-minute mean wind speed,  $V$ , at hub height in the along wind direction and the significant wave height,  $H_s$ .

Another extrapolation procedure is the environmental contour (EC) method [9], a simplified version of the inverse first-order reliability method, which requires one to search for the point of maximum load or response (i.e., the design point) by only considering environmental states defined on an “environmental contour” associated with a target return period. If there are two environmental random variables,  $\mathbf{X} = \{X_1, X_2\}$ , representing wind speed and wave height, as is the case here, then the search domain in a transformed two-dimensional independent standard normal space,  $\mathbf{U}$ , amounts to search on a circle of radius  $\beta$ , the target reliability index corresponding to  $P_T$ . The reader is referred to other studies [3, 7] for details of the environmental contour method applied to wind turbines. It can be easily shown that the environmental contour method essentially approximates the solution for  $l_T$  in Eq. (1) by replacing the conditional distribution of  $L$  given the two-dimensional vector,  $\mathbf{X}$ , by a step function,  $H(f_L(\mathbf{X}))$ , where  $f_L(\mathbf{X}) = L_{med}(\mathbf{X}) - l_T$ , and  $H(y) = 1$ , if  $y > 0$ , and 0 otherwise; also  $L_{med}(\mathbf{X})$  represents the “median” load given  $\mathbf{X}$ . Thus, the EC method does not utilize the full distribution of load given environmental random variables (as established from simulations) but only the median value. It is possible to account for load variability fully by resorting to a search, in this case, of all combinations on a sphere of radius,  $\beta$ , based on the inverse first-order reliability method (inverse FORM); then, the derived load,  $l_T$ , is more accurate and differences between this value and one obtained using direct integration per Eq. (1) result only due to assumed linearization of the limit state function associated with this problem.

## SIMULATION MODEL

A 5MW wind turbine model developed at NREL closely representing utility-scale offshore wind turbines being manufactured today is used in our simulation studies. The turbine is assumed to have a hub height of 90 meters above the mean sea level, and a rotor diameter of 126 meters. The turbine is a variable-speed and collective pitch-controlled machine, with a maximum rotor speed of 12.1 rpm. The rated wind speed is 11.5 m/s. The turbine is assumed to be sited in 20 meters of water and has a monopile support structure, which is assumed to be rigidly connected at the mudline. The turbine is assumed to be installed at an IEC Class 1B wind regime site [1, 10]. A Kaimal power spectrum and an exponential coherence spectrum are employed to describe the turbulence random field over the rotor plane, which is simulated using the computer program, TurbSim [11]. For the hydrodynamic loading on the support structure, irregular linear long-crested waves are simulated using a JONSWAP spectrum [12]. Hydrodynamic loads are computed using Morison’s equation; Wheeler stretching is used to account for the influence of the instantaneous sea surface elevation on

kinematics and hydrodynamics. Stochastic time-domain simulations of the turbine response are performed using the computer program, FAST [13].

## TURBINE RESPONSE

We are interested in the response of the turbine only while it is in an operating state. Accordingly, we perform response simulations for mean wind speeds ranging from cut-in to cut-out wind speeds (i.e., 3 m/s to 25 m/s, here). As a function of the mean wind speed in each simulation, the turbulence intensity is assumed per IEC Class IB site conditions using the Normal Turbulence Model (NTM) [10]. The peak spectral period is modeled as a function of significant wave height based on one year's data from the National Data Buoy Center's Buoy 44007, where the water depth is 19 meters. We discretize the domain of the two environmental random variables using a two-dimensional interval or bin of 2 m/s for mean wind speed and 1 m for significant wave height. We will focus on the out-of-plane blade moment (OoPBM) at the blade root and the fore-aft tower base moment (TBM) at the mudline as the two turbine load variables whose extreme values are of interest in this study.

In order to derive statistics or distributions of turbine loads conditional on wind speed and wave height, multiple simulations have to be carried out for selected pairs of mean wind speed and significant wave height values. Figure 1 shows the average of ten-minute maximum loads from six simulations for each  $V-H_s$  bin considered. It is observed that the maximum out-of-plane blade moment increases with wind speed, up to the rated wind speed of 11.5 m/s, and then decreases, as is expected due to blade-pitch control actions. Also blade loads are seen to be relatively insensitive to wave height. On the other hand, the maximum fore-aft tower base moment, while it also peaks at the rated wind speed, is seen to increase almost linearly with the wave heights.

To investigate the effect of wind on turbine loads in greater detail, we compare the turbine response for mean wind

speeds of 3.7 m/s, 12.1 m/s, and 24.2 m/s, while the significant wave height is held constant at 4.2 m. Figures 2 and 3 suggest that in general blade and tower loads have increased energy (variance) with increasing wind speed. Even though maximum blade moments are higher around the rated wind speed (see Fig. 2(b) and Fig. 1(a)), the variance is smaller there than at 24.2 m/s (Fig. 2(c) and Fig. 3(b)). Tower load variance differences between rated and very high wind speeds are smaller than is the case for blade loads. Important peaks in the power spectra of the loads are seen at 1P (corresponding to the rotor rotation rate of 0.2 Hz at and above the rated wind speed) and multiples as well as at resonant frequencies associated with edgewise and flapwise modes (both of which are present in the OoPBM process) and with tower fore-aft bending.

The effect of waves is studied by comparing the turbine response for significant wave heights of 0.5 m, 4.2 m and 9.4 m, while the mean wind speed is held constant at 12.1 m/s. Figure 4 clearly shows larger peaks in the TBM time series with increasing wave heights. Blade loads are seen to be insensitive to wave height variation. Accordingly, power spectra for tower loads alone are presented in Fig. 5 where no significant influence of wave height is noted, except at frequencies below around 0.2 Hz where wave energy is dominant, with sea surface elevation peak spectral frequencies being 0.14, 0.10 and 0.08 Hz for significant wave heights of 0.5, 4.2 and 9.4 m, respectively.

Table 1 summarizes statistics of the blade and tower loads obtained from six simulations each for the wind and wave conditions discussed in Figs. 2-5. OoPBM statistics, as was discussed before, are insensitive to wave height. Also, the mean, SD (standard deviation), and maximum OoPBM are all systematically higher around the rated wind speed compared to other wind speeds. Interestingly, too, the skewness, kurtosis, and peak factor are seen to vary greatly with wind speed; peak factors are lowest around rated wind speed.

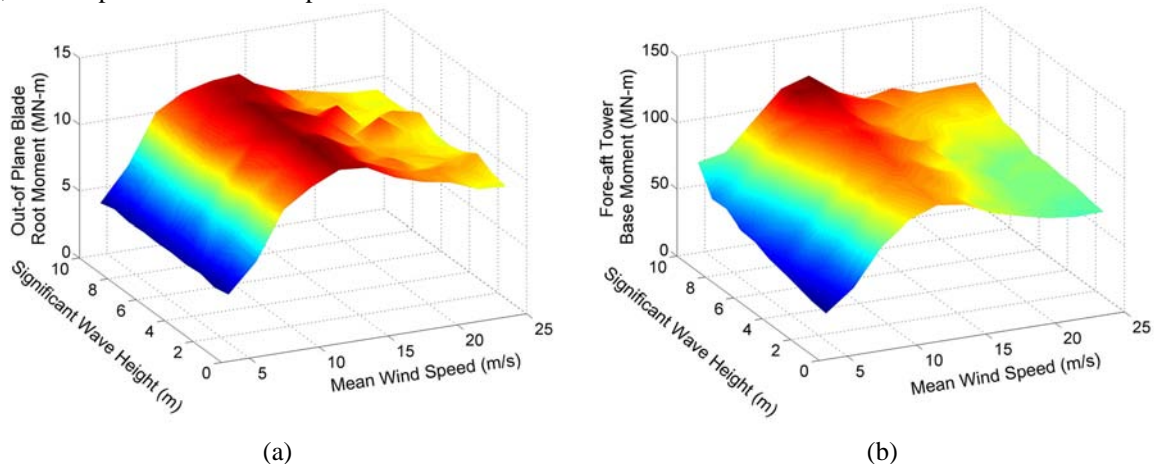


Figure 1. Variation with mean wind speed and significant wave height of the mean of the maximum values from six simulations of (a) the out-of-plane blade root moment; and (b) the fore-aft tower base moment.

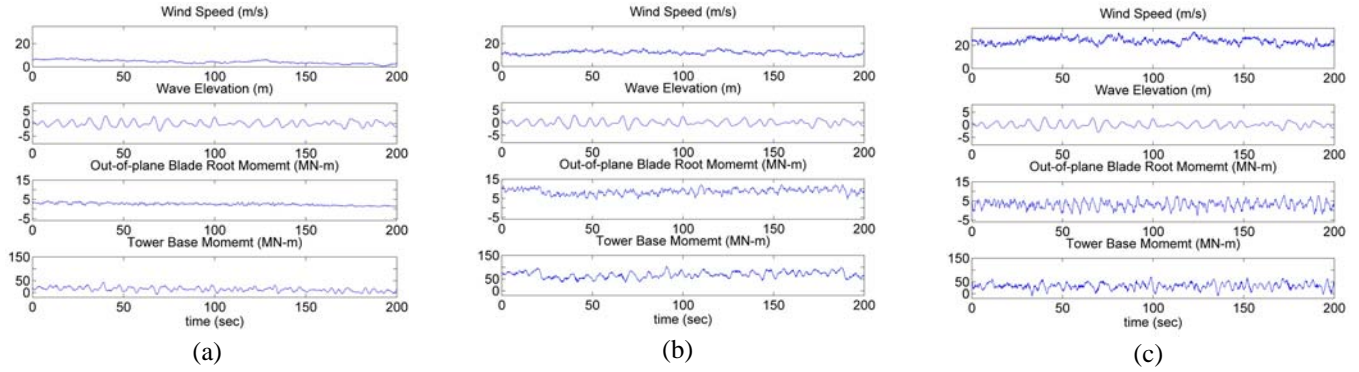


Figure 2. Representative time series of wind speed, sea surface elevation, out-of-plane blade moment, and tower bending moment for mean wind speeds of (a) 3.7 m/s, (b) 12.1 m/s and (c) 24.2 m/s. The significant wave height is fixed at 4.2 m.

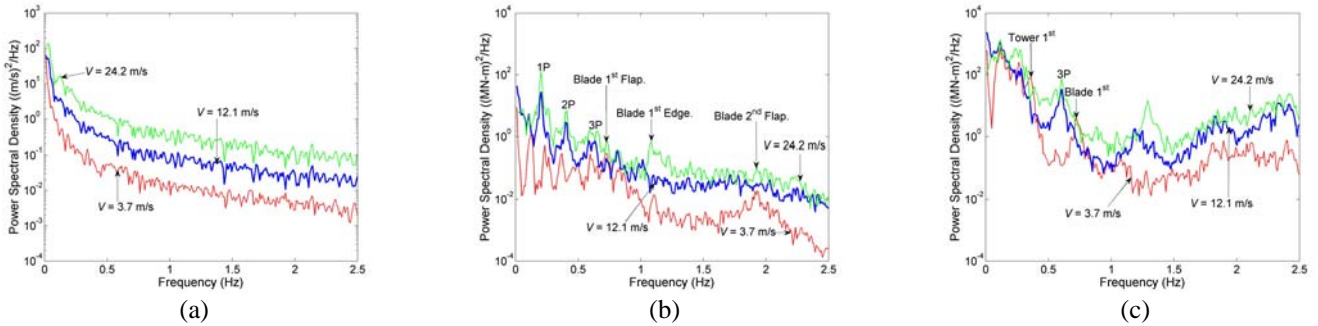


Figure 3. Variation of power spectral density with mean wind speed for (a) wind speed, (b) out-of-plane blade moment, and (c) tower bending moment. The significant wave height is fixed at 4.2 m.

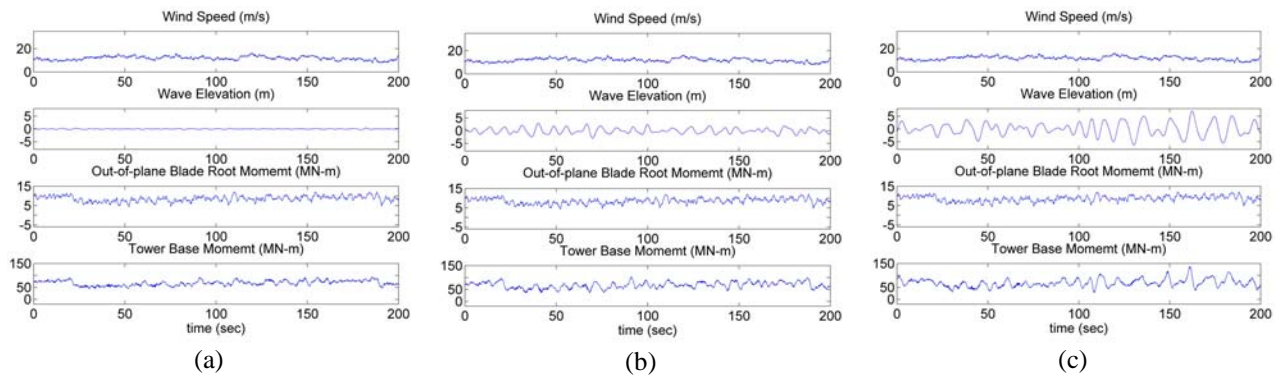


Figure 4. Representative time series of wind speed, sea surface elevation, out-of-plane blade moment, and tower bending moment for significant wave heights of (a) 0.5 m, (b) 4.2 m and (c) 9.4 m. The mean wind speed is fixed at 12.1 m/s.

Table 1. Ten-minute statistics of turbine loads for different wind speed and wave height bins.

V (m/s)	$H_s$ (m)	Out-of-plane moment at the blade root						Fore-aft tower base moment					
		Max	Mean	SD	Skew.	Kurt.	PF	Max	Mean	SD	Skew.	Kurt.	PF
		(all in MN-m)						(all in MN-m)					
12.0	0.5	12.5	8.2	1.5	-0.05	2.64	2.85	97.3	65.2	10.9	0.11	2.41	2.96
12.0	4.5	12.7	8.3	1.6	-0.25	2.74	2.80	106.6	66.3	12.7	-0.03	2.76	3.17
12.0	9.5	12.2	8.2	1.5	-0.14	2.61	2.60	124.2	66.2	16.1	0.18	3.08	3.61
4.0	4.5	4.5	2.3	0.6	0.49	2.83	3.65	39.4	12.3	8.6	0.07	2.79	3.16
12.0	4.5	12.7	8.3	1.6	-0.25	2.74	2.80	106.6	66.3	12.7	-0.03	2.76	3.17
24.0	4.5	9.3	3.0	2.0	-0.14	2.89	3.07	78.4	32.8	12.3	0.07	3.07	3.73

Note: V: Mean wind speed,  $H_s$ : Significant wave height, Max: Ten-minute maximum, SD: Standard deviation, Skew.: Skewness, Kurt.: Kurtosis, PF: Peak Factor = (Max – Mean)/SD.

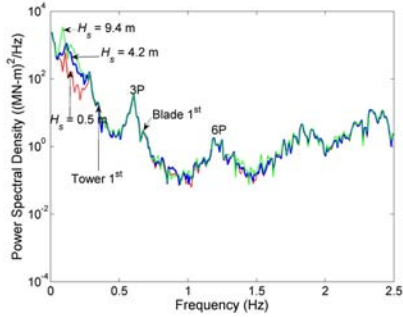


Figure 5. Variation of power spectral density of fore-aft tower bending moment with significant wave height. The mean wind speed is fixed at 12.1 m/s.

The TBM process statistics are also interesting—when studied with variation in wave heights, it is seen that mean and SD levels change only very slightly, yet maximum values change to a greater degree suggesting that the loads processes have significant differences in higher-order moments and associated peak factors, also reflecting different degrees of non-Gaussian character as a function of wave height.

From the preceding results, it can be concluded that: (1) blade and tower loads are largest around the rated wind speed, but peak factors are lowest there; (2) blade loads are independent of wave height; and (3) maximum tower loads increase systematically with wave height. Hence, turbine design loads are expected to be governed either by mean wind speeds near rated (as the mean, SD, and maximum response are all higher there) or by higher-than-rated wind speeds where larger variability in loads and associated large peak factors could lead to large extreme values. Also, tower design loads are likely to result from larger wave heights.

### SHORT-TERM EXTREME LOAD DISTRIBUTIONS

The short-term distribution of turbine extreme loads,  $F_{L|X}(l)$ , which enables prediction of long-term loads for design according to Eq. (1), requires data on load extremes. The global maximum and peak-over-threshold methods are commonly used to extract load extremes from time series data. We use the peak-over-threshold method here, as it can provide a large number of load extremes from a given number of simulations, resulting in better definition of distribution tails which is important when extrapolating loads to rare fractiles or low probability of exceedance levels.

In the peak-over-threshold (POT) method, the maximum load from each segment of a time series that lies between two successive upcrossings of a chosen threshold is retained as a load extreme. While the choice of threshold may be optimized [4], here we choose a threshold fixed at a mean plus 1.4 SD level [2]. The mean and standard deviation used are based on all the load time series simulations carried out for a wind speed and wave height bin ( $X$ ). The cumulative distribution function for load extremes,  $F_{L|X=x}(l)$  is:

$$F_{L|X=x}(l) = \left[ F_{L_{POT}|X=x}(l) \right]^n \quad (2)$$

where  $n$  is the expected number of peaks (above the chosen threshold) in ten minutes, and  $F_{L_{POT}|X=x}(l)$  represents the cumulative distribution function of POT-based load extremes. This distribution is established non-parametrically here since distribution tails from a limited number of simulations—six, here—are not stable enough to allow parametric model fits.

Equation 2 is based on the assumption that the peaks above the chosen threshold in a bin are independent. If a load non-exceedance level of probability,  $p$ , is of interest, the corresponding load fractile,  $l_p$ , based on the POT distribution, is associated with a non-exceedance probability,  $p^{1/n}$ , and may be estimated as:

$$l_p = F_{L_{POT}|X}^{-1} \left[ p^{1/n} \right] \quad (3)$$

Note that as the selected threshold level is increased, the expected number of peaks that are retained decreases, and when this number is unity, the POT method approaches the global maximum method, since then on average, one peak is extracted from each simulation. For typical threshold levels, the expected number of retained peaks is significantly larger than unity and, as a result,  $p^{1/n}$  can approach values that are close to unity. As an example, if the expected number of peaks above a chosen threshold is 80, then the non-exceedance fractile level for POT data corresponding to the ten-minute median extreme load is  $0.5^{1/80} = 0.99137$ . If loads corresponding to this probability level are to be established non-parametrically from simulations, at least  $1/(1 - 0.99137)$  or 116 peak values above the chosen threshold must be available for the wind speed and wave height bin representing  $X$ . For tight confidence intervals on such rare load levels, the number of peaks (and thus simulations) might even need to be an order of magnitude higher. Note that extrapolation may often be required then for two reasons: (1) to estimate rarer fractiles (such as, say, the 80<sup>th</sup> percentile of the ten-minute extreme load instead of the median) as the minimum number of required data may exceed the amount of POT data available from limited simulations; and (2) to have tight confidence intervals on predicted POT load fractiles. Extrapolation is discussed further when addressing long-term loads in the context of the inverse first-order reliability method.

### LONG-TERM LOADS

With the inverse first-order reliability method, long-term loads may be estimated by using simulations to establish the full conditional distribution for the turbine load variable given wind speed and wave height and then turning the integral equation of Eq. (1) into a search for the maximum load on a locus of points in a 3-D space (representing,  $V$ ,  $H_s$ , and  $L$ ) associated with the target failure probability. A reduced effort, though less exact, is possible with the environmental contour method where the 3-D locus searched is reduced to a 2-D one and, additionally, only the conditional median value of  $L$  given  $V$  and  $H_s$  must be estimated for points on the locus rather than the full distribution.

Table 2: Comparison of 20-year design loads for blade and tower loads estimated by different methods, when load extremes data are based on the peak-over-threshold method

Method	20-year design for OoPBM			20-year design for TBM		
	$V$	$H_s$	OoPBM	$V$	$H_s$	TBM
	m/s	m	MN-m	m/s	m	MN-m
2-D Environmental Contour	12.0	6.2	12.8	12.0	6.2	105.2
2-D Environmental Contour with corrections	12.0	6.2	13.2	12.0	6.2	107.9
3-D Inverse First-Order Reliability Method	14.0	5.5	13.6	16.0	5.5	119.9

We first estimate long-term design loads using the 2-D formulation, also referred to as the environmental contour method. Then, we compare 2-D design loads with those obtained from a full 3-D inverse reliability approach. We start by using six ten-minute turbine response simulations for each environmental state to establish turbine load statistics, and subsequently investigate the effect of number of simulations on design load predictions. All the design loads discussed hereinafter correspond to a return period of 20 years.

To derive long-term loads at the site of interest, we require information on the joint distribution of environmental random variables. For the IEC Class 1B wind regime (for which our turbine model is being considered), we assume that the ten-minute mean wind speed,  $V$ , at hub height has an average value of 10 m/s and that it can be described by a Rayleigh distribution. We choose to truncate this distribution below the cut-in wind speed of 4 m/s and above the cut-out wind speed of 24 m/s, since we are interested only in studying turbine loads during operation. The significant wave height,  $H_s$ , conditional on the mean wind speed, is assumed to be represented by a two-parameter Weibull distribution. The expected value of  $H_s$  given  $V$  is based upon the JONSWAP correlation between wind and waves [12], while a coefficient of variation for  $H_s$  given  $V$  is assumed to be constant at 0.2.

### **The 2-D Environmental Contour (EC) Method**

In the 2-D formulation with the EC method, the median turbine load given  $X$  is required. It is obtained from POT data by setting  $p$  to be 0.5 in Eq. (3). The estimated 20-year design loads are presented in Table 2. The OoPBM design load is 12.8 MN-m which is associated with a mean wind speed of 12 m/s and a significant wave height of 6.2 m. The TBM design load is 105.2 MN-m and it also results from the same wind speed and wave height. That the “design” wind speed is close to the rated wind speed is expected as median extreme turbine loads are largest there, as was discussed earlier. The design wave height of 6.2 meters is the larger of the two possible wave heights on the 20-year environmental contour that accompanies the mean wind speed of 12 m/s.

Table 3: Required fractiles for the design environmental states for the 2-D environmental contour method.

Load	Average number of peaks, $n$	Required fractile, $0.5^{1/n}$	Largest empirical fractile
OoPBM	87.2	0.9921	0.9981
TBM	80.2	0.9914	0.9979

The accuracy of the derived EC design loads may be evaluated by determining whether the desired fractile for the POT load requires extrapolation, given the number of peaks above the threshold retained from six simulations. Table 3 shows that for both blade and tower loads, the required POT fractiles are smaller than the largest available empirical fractile,  $1-1/(6n+1)$ . This suggests that extrapolation is not necessary to arrive at turbine design loads with the EC method; nevertheless, the method has accuracy limitations both because it does not employ the full distribution of turbine loads conditional on  $X$  and because even the non-extrapolated fractile is subject to statistical uncertainty due to limited data. To assess both these sources of inaccuracy, we estimate design loads using direct integration. We model the conditional load distribution in Eq. (1) as a step function that attains a unit value at the median load. To yield the desired probability of failure, the design loads are found to be 12.7 MN-m and 110.2 MN-m, respectively, for OoPBM and TBM, which are very close to those obtained from the environmental contour method. Hence, we conclude that the EC method is not grossly inaccurate relative to an exact integration approach that works with the same data. Still, there are other reasons why the EC-based design loads might not be correct; these reasons have to do with incomplete modeling of the conditional distribution of turbine loads given wind speed and wave height. This is addressed next.

### **Correction to the EC Design Loads**

While the full distribution of loads (given environmental conditions) can be employed in a 3-D inverse FORM approach, this requires far more computational effort. An alternative strategy is to apply a correction to the 2-D EC design loads [14], as has been successfully applied for onshore turbine design loads [4]. This correction accounts for (1) response variability, at a given environmental state ( $X$ ), by quantitative comparison of different fractiles of the load at the EC design point, and (2) background variability which reflects sensitivity of the EC design load to changes in the return period from the original value (20 years). After applying this correction, design loads are estimated to be 13.2 MN-m and 107.9 MN-m for OoPBM and TBM, respectively (see Table 2). Response variability is largely responsible for the change in design loads here. However, the corrected blade and tower design loads are only about 3% larger than the 2-D EC values.

### 3-D Inverse FORM

If instead of only seeking the median extreme load given  $X$ , the full probability distribution of the turbine extreme load,  $L$ , is established by simulations, a search is needed for the maximum value of a different  $p_3$  fractile on load extremes consistent with each environmental state ( $V, H_s$ ) and with the specified target probability of failure,  $P_T$  (or associated reliability index,  $\beta$ , where  $\Phi(-\beta) = P_T$ ):

$$p_3 = \Phi \left[ \beta^2 - \left( \Phi^{-1}(F_V(v)) \right)^2 - \left( \Phi^{-1}(F_{H|V}(h)) \right)^2 \right]^{\frac{1}{2}} \quad (4)$$

where  $\Phi(\cdot)$  and  $\Phi^{-1}(\cdot)$  refer to the standard normal cumulative and inverse cumulative distribution functions, respectively, and  $F_V(v)$  and  $F_{H|V}(h)$  refer to the cumulative distribution functions for wind speed and for significant wave height (given wind speed), respectively. For POT data, the load fractiles are estimated according to Eq. (3). Note that with the EC method, effectively,  $p_3$  is the median (i.e.,  $p_3 = 0.5$ ).

With this 3-D inverse FORM approach, the design loads (here obtained by searching only on gridded  $V$ - $H_s$  pairs where simulations were carried out) are 13.6 MN-m and 119.9 MN-m for the blade and tower loads, respectively (see Table 2). These same loads are obtained using direct integration method, which establishes the accuracy of the 3-D inverse FORM results. These 3-D design loads are roughly 6% and 14% larger, respectively, for the blade and tower loads than those obtained with the 2-D method. Interestingly, the design wind speed with the 3-D formulation, which is 14 m/s for the blade load and 16 m/s for the tower load, is no longer near the rated wind speed, as was the case with the 2-D formulation. This implies that the full conditional load variability (as a function of wind speed and wave height) is important.

Note that for a pitch-controlled turbine, the rated wind speed is expected to be the design wind speed. Furthermore, in order to reduce the simulation effort, a limited number of wind speeds (as few as three), near rated, may be selected for

simulations, as is also suggested in Annex G of the draft IEC guidelines for offshore wind turbines [1]. If we used this criterion, with a small wind speed bin size of 1 m/s, we might miss design wind speeds of 16 m/s that were found here. Ignoring load variability may lead to misleading design loads.

We should note that the 2-D EC design loads and the 3-D inverse FORM design loads were calculated based on simulations for a discrete set of gridded values of  $V$  and  $H_s$ . In subsequent discussions, we examine the environmental state (i.e.,  $V$  and  $H_s$  values) at the 3-D design point in Table 2. For the blade and tower loads, these environmental states correspond, respectively, to  $V = 14$  m/s,  $H_s = 5.5$  m and  $V = 16$  m/s,  $H_s = 5.5$  m in the 3-D approach, are studied in greater detail in the following.

In order to assess the accuracy of estimated  $p_3$ -load fractiles for the design environmental state in this 3-D inverse FORM approach, it is useful to first determine if the required fractile needed to be extrapolated from the POT data. Table 4 shows that for both loads the required POT fractiles are significantly higher than the largest available empirical fractile. In our non-parametric model for load distributions, we assume saturation of the tail and somewhat simplistically estimate the required fractile as the largest observed value. The load distribution (Fig. 6), however, shows that the assumption of saturation of tails cannot be justified. As a result, 3-D inverse FORM design loads based on this non-parametric approach here are clearly low and unconservative.

Table 4: Required fractiles for design environmental states for the 3-D inverse FORM approach.

Load	Required load fractile, $p_3$	Average no. of peaks, $n$	Required fractile for POT, $p_3^{1/n}$	Largest empirical fractile
OoPBM	0.99998997	66.2	0.99999985	0.9975
TBM	0.99999613	74.2	0.99999995	0.9978

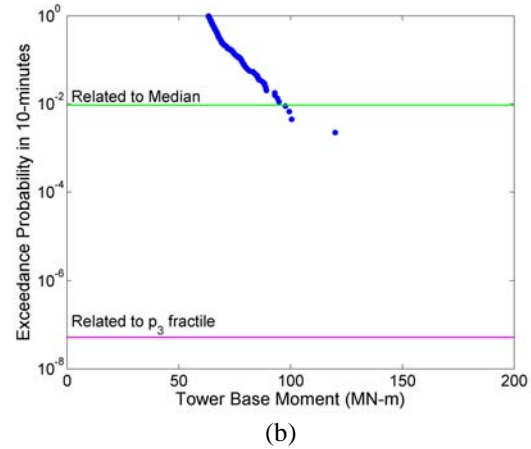
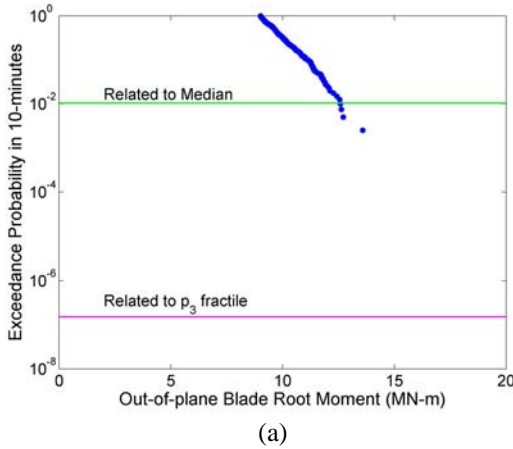


Figure 6. Load distributions of the POT data for governing environmental states based on 6 simulations for (a) a mean wind speed of 14 m/s and significant wave height of 5.5 m for OoPBM; and (b) a mean wind speed of 16 m/s and a significant wave height of 5.5 m for TBM.

## Control Actions and Number of Simulations

An interesting aspect that may be seen from Fig. 6 is that the maximum observed load value, which determines the required extrapolated fractile, is significantly larger than other load values in the tail of distribution. To investigate what conditions bring about this large load, we study in Fig. 7 relevant time histories of wind speed, OoPBM, and TBM series along with that of blade pitch angle for a single ten-minute simulation (out of six for the design bin) that included this large load. The maximum loads were seen to occur when the blade pitch angle suddenly reduced to zero at time instants of roughly 20 sec, 100 sec, and 175 sec. This is due to the control system for this pitch-controlled turbine, which is such that the blade starts to pitch when the instantaneous wind speed exceeds the rated wind speed of 11.5 m/s. At instants when the wind speed falls below rated, the pitch angle reduces to zero, and if the wind speed increases before the blade can pitch back, large loads result.

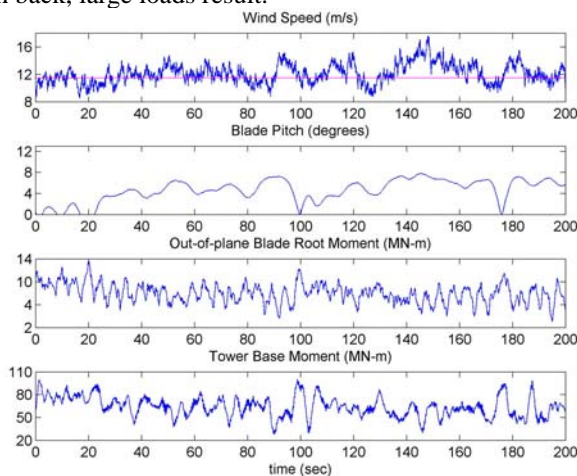


Figure 7. Time series of wind speed, blade pitch, OoPBM, and TBM for a mean wind speed of 14 m/s and significant wave heights of 5.5 m.

Since these large loads due to control actions are observed only in one out of six simulations, the distribution tails may only saturate and have better definition than in Fig. 6 if more such large load values result upon performing more simulations. We therefore carry out more simulations for the governing environmental states and find that at least 60 and 150 simulations, respectively, are needed for the blade and tower loads. The corresponding distributions, shown in Fig. 8, also illustrate how the distribution tails fill in, and hence become more reliable. Clearly, due to blade pitch-control actions, performing only six simulations per environmental state may be inadequate to obtain reliable distributions by means of parametric model fits to the data; this is why non-parametric fractiles were employed with the 2-D and 3-D approaches that were based on only six simulations.

With the more reliable POT load distribution tails possible only due to the larger number of simulations, we

attempt fits with parametric models. With a two-parameter Weibull distribution on the tails and a least squares basis, Figs. 9a and 10a shows that for the required fractiles of Table 4, loads of 15.3 MN-m and 147.1 MN-m result for the blade and tower loads, respectively. These loads are about 13% and 23% larger for blade and tower loads, respectively, than those from the non-parametric approach and based on only six simulations. This is expected since the non-parametric unconservatively assumed saturation of distribution tails. As seen, a large number of simulations is required to yield reliable distribution tails and more accurate design loads.

## COMPARISON OF POT AND GLOBAL MAXIMA

In the preceding discussions, we used the peak-over-threshold (POT) data to extract load extremes. An alternative approach is to use global (or epochal) maxima in which only statistics of the single largest load value from each simulation are used. It is of interest to examine how design load predictions differ from the two methods. We fit two-parameter Weibull distributions to the tails of global maxima data for the design environmental states, and estimate load fractiles required with the 3-D inverse FORM approach. Figures 9b and 10b show these fits for the blade and tower loads, respectively. Design load predictions obtained using the global maxima method are 14.5 MN-m and 136.6 MN-m for the blade and tower load, respectively; they differ only slightly from those obtained with the POT method with parametric distribution fits (Fig. 9a and 10a). Larger differences in predictions for the tower loads are likely due to relatively poor distribution fits with both methods.

Finally, an important issue when using the POT method is related to the selection of threshold. As the threshold level is increased, the number of peaks decreases and, at an appropriately high threshold, the POT method may result in the same number of load extremes, on average, as the global maxima method. We now estimate required fractiles for the governing environmental state with the 3-D inverse FORM approach using different thresholds and two-parameter Weibull parametric fits for POT distribution tails. Table 5 shows computed fractiles for blade and tower loads. For blade loads, it can be seen that the variation in load fractiles with different thresholds is not significant. The reason is that very good parametric fits, such as those shown in Fig. 9a, are obtained for all threshold levels. For tower loads, the required load fractiles show slightly greater variation with different threshold choices which may be partly due to less evident and stable trends in distribution tails for these loads (as seen, for example, in Fig. 10a). Based on these observations, we conclude that the agreement between design loads using the POT and global maxima methods is generally good and is independent of threshold choice as long as distribution tails are reliable enough to allow a good parametric fit.



Figure 8. Load distributions of the POT data for governing environmental states based on (a) 60 simulations of OoPBM for a mean wind speed of 14 m/s and a significant wave height of 5.5 m; and (b) 150 simulations of TBM for a mean wind speed of 16 m/s and a significant wave height of 5.5 m.

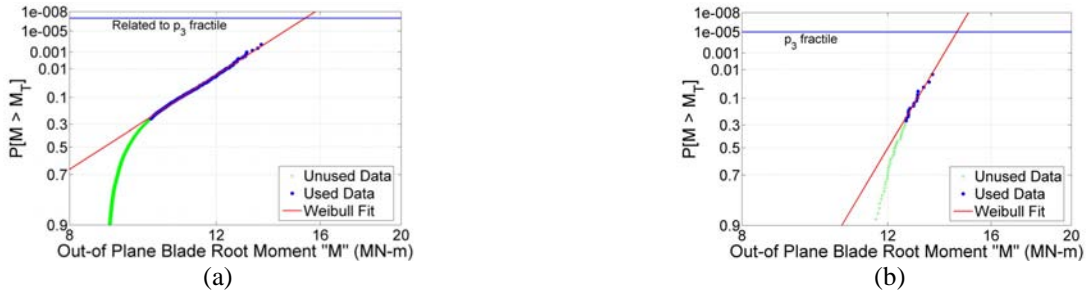


Figure 9. Two-parameter Weibull distribution fits (a) to POT data, and (b) to global maxima data based on 60 simulations with a mean wind speed of 14 m/s and a significant wave height of 5.5 m for out-of-plane blade moment.

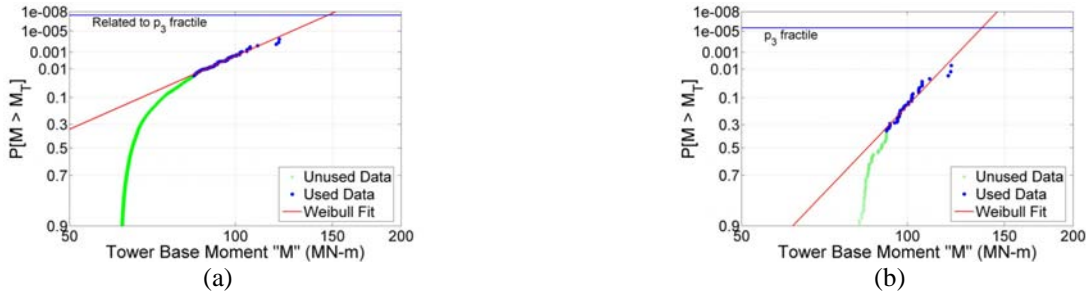


Figure 10. Two-parameter Weibull distribution fits (a) to POT data, and (b) to global maxima data based on 150 simulations with a mean wind speed of 16 m/s and a significant wave height of 5.5 m for fore-aft tower base moment.

Table 5: Effect of threshold level on the estimate of load fractile for the design environmental state for OoPBM ( $p_3 = 0.99998997$ ) and TBM ( $p_3 = 0.99999613$ ). Threshold = Mean +  $N_\sigma \times$  (Standard deviation)

Threshold Level, $N_\sigma$	OoPBM ( $V = 14$ m/s, $H_s = 5.5$ m)			TBM ( $V = 16$ m/s, $H_s = 5.5$ m)		
	Ave. no. of peaks, $n$	Required exceedance probability, $1 - p_3^{1/n}$	Load fractile (MN-m)	Ave. no. of peaks, $n$	Required exceedance probability, $1 - p_3^{1/n}$	Load fractile (MN-m)
1.4	66.8	$1.50 \times 10^{-7}$	15.3	85.6	$4.52 \times 10^{-8}$	147.1
1.7	44.7	$2.24 \times 10^{-7}$	14.9	56.4	$6.86 \times 10^{-8}$	148.1
2.0	28.9	$3.47 \times 10^{-7}$	14.8	34.9	$1.11 \times 10^{-7}$	145.9
2.3	17.1	$5.86 \times 10^{-7}$	14.7	20.2	$1.91 \times 10^{-7}$	143.0
2.7	8.1	$1.23 \times 10^{-6}$	14.6	9.7	$3.97 \times 10^{-7}$	139.7
3.0	4.0	$2.51 \times 10^{-6}$	14.6	4.9	$7.97 \times 10^{-7}$	142.4
MAX	1.0	$1.00 \times 10^{-5}$	14.5	1.0	$3.87 \times 10^{-6}$	136.6

## CONCLUSIONS

Our objective in this study was to derive long-term design loads for a utility-scale 5MW offshore wind turbine sited in 20 meters of water. The focus was on the out-of-plane blade bending moment at a blade root and the fore-aft tower base moment at the mudline. Load extremes data needed to establish short-term load distributions were extracted from time series of turbine response simulations using the peak-over-threshold method. Design loads were estimated using 2-D and 3-D inverse first-order reliability method approaches (the former is also referred to as the environmental contour or EC method) and compared with direct integration. The following are general conclusions for the offshore wind turbine studied:

- The EC method is efficient compared to direct integration but design load predictions are based on limited consideration for turbine response variability and can be inaccurate and unconservative.
- The variability in turbine loads for a given environmental state is found to be significant, due to which design loads based on median values (2-D EC method) of loads given mean wind speed and significant wave height are smaller than those based on higher-than-median fractiles (3-D inverse FORM).
- Importantly, the design wind speed is not the rated wind speed (as is often the case) but is above rated when load variability is considered.
- A chief source of load variability results from blade-pitch control actions that result in large loads such that the tails of the short-term load distribution are not reliable unless a large number of simulations are performed.

While the above results are based on the peak-over-threshold method, a comparison of predictions based on the global maxima and POT methods were close as long as distribution tails are reliable and well defined.

These conclusions, while particular to the turbine model studied, are useful to consider for any simulation-based exercise that seeks to predict design loads for extreme (ultimate) limit states. This study also suggests that the effect of control actions on extreme loads needs careful study; in particular it is of interest to investigate methods to account for variability due to control actions since such they can alter the tails of load distributions in different ways than loads that result from uncontrolled turbine states.

## ACKNOWLEDGMENTS

The authors gratefully acknowledge the financial support provided by a CAREER Award (No. CMS-0449128) from the National Science Foundation and by Contract No. 30914 from Sandia National Laboratories. They also acknowledge assistance from Mr. Jason Jonkman at the National Renewable Energy Laboratory with the wind turbine simulation model used in this study.

## REFERENCES

- [1] IEC 61400-3, 2005, Wind Turbines – Part 3: Design Requirements for Offshore Wind Turbines, Intl. Electrotechnical Commission, TC88 WG3 Committee Draft.
- [2] Moriarty, P. J., Holley, W. E. and Butterfield, S. P., 2004, Extrapolation of Extreme and Fatigue Loads using Probabilistic Methods, National Renewable Energy Laboratory, NREL/TP-500-34421, Golden, CO.
- [3] Saranyasoontorn, K. and Manuel, L., 2006, “Design Loads for Wind Turbines using the Environmental Contour Method,” *Journal of Solar Energy Engineering*, Transactions of the ASME, Vol. 128, No. 4, pp. 554-561.
- [4] Ragan, P. and Manuel, L., 2007, “Statistical Extrapolation Methods for Estimating Wind Turbine Extreme Loads,” *Proc. ASME Wind Energy Symposium*, AIAA, Reno, NV.
- [5] Cheng, P. W., 2002, A Reliability based Design Methodology for Extreme Response of Offshore Wind Turbines, *PhD Dissertation*, Delft Univ. of Technology, The Netherlands.
- [6] Norton, E., 2004, Investigation into IEC Offshore Draft Standard Design Load Case 1.1, Recommendations for Design of Offshore Wind Turbines, Risø National Laboratory, Denmark.
- [7] Saranyasoontorn, K. and Manuel, L., 2005, “On Assessing the Accuracy of Offshore Wind Turbine Reliability-Based Design Loads from the Environmental Contour Method,” *Intl. J. of Offshore and Polar Engrg.*, Vol. 15, No. 2, pp. 132-140.
- [8] Tarp-Johansen, N. J., 2005, Extrapolation including Wave Loads – Replacing the Distribution of  $H_s$  by a Suitable Percentile, Recommendations for Design of Offshore Wind Turbines, Risø National Laboratory, Denmark.
- [9] Winterstein, S. R., Ude, T. C., Cornell, C. A., Bjerager, P. and Haver, S., 1993, “Environmental Contours for Extreme Response: Inverse FORM with Omission Factors,” *Proceedings, ICOSSAR-93*, Innsbruck.
- [10] IEC 61400-1, 2005, Wind Turbines – Part 1: Design Requirements, Intl. Electrotechnical Commission, Ed. 3.
- [11] Jonkman, B. J. and Buhl, M. L. Jr, 2007, TurbSim User’s Guide, National Renewable Energy Laboratory, NREL/TP-500-41136, Golden, CO.
- [12] Chakrabarti, S. K., 1987, Hydrodynamics of Offshore Structures, WIT Press, UK.
- [13] Jonkman, J. M. and Buhl, M. L. Jr, 2005, FAST User’s Guide, National Renewable Energy Laboratory, NREL/EL-500-38230, Golden, CO.
- [14] Winterstein, S. R. and Engebretsen, K., 1998, “Reliability-based Prediction of Design Loads and Responses for Floating Ocean Structures,” *International Conference on Offshore Mechanics and Arctic Engineering*, Lisbon.